

Separation of Forward-Backward Waves in the Arterial System using Multi-Gaussian Approach from Single Pulse Waveform

Rahul Manoj, Raj Kiran V, Nabeel P M, *Member IEEE*, Mohanasankar Sivaprakasam and Jayaraj Joseph

Abstract— The arterial pulse waveform has an immense wealth of information in its morphology yet to be explored and translated to clinical practice. Wave separation analysis involves decomposing a pulse wave (pressure or diameter waveform) into a forward wave and a backward wave. The backward wave accumulates reflections due to arterial stiffness gradient, branching and geometric tapering of blood vessels across the arterial tree. The state-of-the-art wave separation analysis is based on estimating the input impedance of the target artery in the frequency/time domain, which requires simultaneously measured or modelled flow velocity and pressure waveform. We are proposing a new method of wave separation analysis using a multi-gaussian decomposition. The novelty of this approach is that it requires only a single pulse waveform at the target artery. Our method was compared against the triangular waveform-based impedance method. We successfully separated forward and backward waveform from the pressure waveform with maximum RMSE less than 5 mmHg and mean RMSE of 1.31 mmHg when compared against the triangular flow/impedance method. Results demonstrated a statistically significant correlation ($r > 0.66$, $p < 0.0001$) for Reflection Magnitude (RM) and Reflection Index (RI) for the multi-gaussian approach against the triangular flow method for 105 virtual subjects. The range of RM was from 0.35 to 0.97 (RI: 27.53% to 49.29%). This method proves to be a technique for evaluating reflection parameters if only a single pulse measurement is available from any artery.

Clinical Relevance— This simulation study supplements the evidence for wave reflections. It provides a new method to study wave reflections using only a single pulse waveform without the need for any measured or modelled flow.

I. INTRODUCTION

An arterial pulse waveform is a superposition of a forward and a backward wave. The backward wave or reflections are an integral part of the arterial conduct system that helps to maintain the homeostasis between elastic, muscular and micro blood vessel circulations. Pulse Pressure (PP) is one parameter measured in a clinical setting that is directly influenced by wave reflections [1]. As reported in several studies, PP

amplifies from central to peripheral arteries and the clinical implication of this phenomenon is well noted in diverse clinical and epidemiological research [2]. This PP amplification is a consequence of arterial geometry (tapering and branching) and stiffness gradient along the arterial tree, resulting in wave reflections modifications. The effect of wave reflections on pulse waveforms is attributed to their magnitude and time of return. As the reflected waves arrive before systole, augmenting it, increasing the PP, impacting cardiac afterload, coronary heart disease, stroke and end-organ tissue perfusion [3].

The ability to quantify the magnitude and return time of wave reflections could advance the cardiovascular risk stratification methodologies [4]–[8], and this can be directly obtained by analyzing pulse waveforms (diameter or pressure). Although the augmentation index (AIx) is one of the conventional measures to quantify reflections, it relies not only on the wave reflection magnitude but also on morphologic and temporal parameters of the incident and reflected waves [9]. A more proper way to quantify the amount of reflection involves separating pulse waveforms into forward and backward waveforms. The state-of-the-art technique in wave separation can be performed in the frequency domain [10] and in the time domain [11] based on characteristic impedance. Both the methods involve simultaneous measurement flow (or flow velocity) and pressure waveform from the same arterial site. Challenges associated with multi-modal signal acquisition involves measuring time-synchronized, frequency matched signals with the same sampling rate and the practical difficulty in ensuring single site measurement due to the form factor of sensors used [12]–[14], limits the utility of wave separation methods in a clinical setting. Therefore wave separation methods that use a modelled or assumed flow velocity have the advantage that only a single pulse measurement is required. But these techniques come with their limitations. In modelled flow [15], extensive population data was used to arrive at an average flow waveform that was used for analysis and in [16], a modified version of the characteristic impedance method that uses an un-calibrated and assumed triangular flow waveform instead of the measured flow which is subjected to changes in fiducial points on the pulse morphology. In a slightly different approach, a tube load model-based separation of pressure waves [17] is performed using a proximal and distal measurement of pressure wave alone. Still, this technique ignores wave reflections due to arterial stiffness, tapering, branching and modelled the reflections due to peripheral resistance.

Rahul Manoj and Raj Kiran V are with the Electrical Engineering Department, Indian Institute of Technology Madras, Chennai-600036, India (e-mail: rahulmanojktym@gmail.com).

Nabeel P M is with Healthcare Technology Innovation Centre (HTIC), Indian Institute of Technology Madras Research Park, Chennai-600113, India.

Jayaraj Joseph is with the faculty of Electrical Engineering Department. Mohanasankar Sivaprakasam is the Director of Healthcare Technology Innovation Centre and with the faculty of Electrical Engineering Department at Indian Institute of Technology Madras, Chennai-600036, India

To account for the challenges mentioned above, we have developed a method that relies on a single pulse waveform and does not require any modelled or measured flow velocity waveform. The new modelling approach uses multi-Gaussian decomposition to separate forward and backward waves from the parent pulse waveform. Our method was compared against a method that requires only a single pulse waveform that uses a triangular flow-based impedance approach.

II. METHODS

A. Theory – Multi-Gaussian Decomposition

The pressure cycle ($P(t)$) after removal of DC offset (DC_{OFF}), ($P(t)$ becomes pulse pressure cycle, $P_P(t)$), is the input to this multi-Gaussian modelling approach. The non-linear model consists of the sum of N Gaussian curves, with their respective amplitudes (A_i , $i = 1$ to N), mean locations (M_i , $i = 1$ to N) and standard deviation locations from respective means (C_i , $i = 1$ to N) on the time axis, expressed as in (1).

$$G(K, t) = \sum_{i=1}^N A_i e^{-\frac{1}{2} \times \frac{(t-M_i)^2}{C_i^2}} \quad (1)$$

Where $G(K, t)$ is the modelled pressure waveform, K is the parameter set consisting of A_i , M_i and C_i ; t is the time axis. This non-linear multi-Gaussian model was fit for the pulse pressure cycle. For robust curve fitting Levenberg-Marquardt (LM) algorithm was applied, with K as the set of parameters

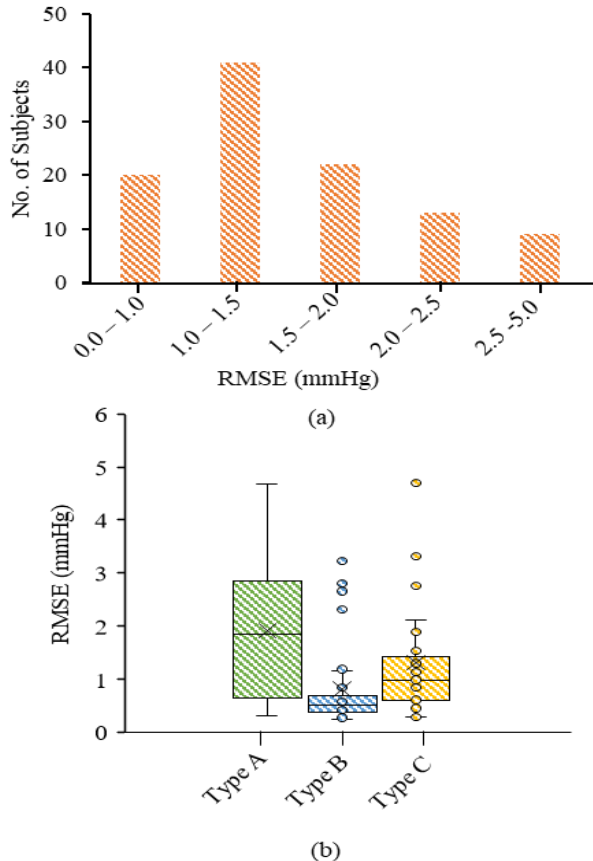


Fig.2. (a) Bar-chart of RMSE for 105 subjects, (b) RMSE for Type A, Type B and Type C subjects

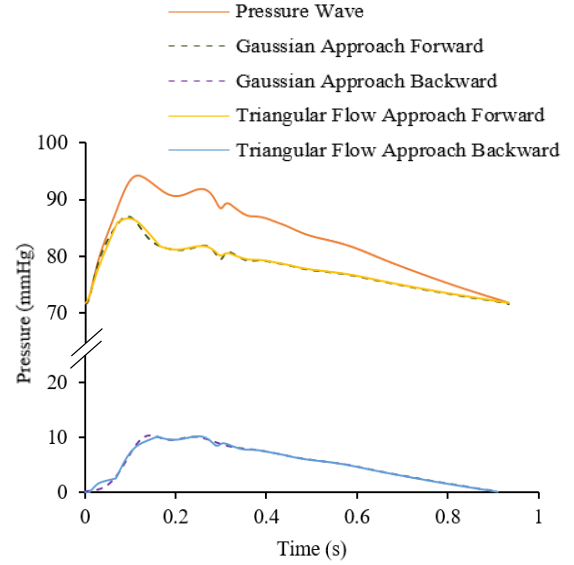


Fig.1. Wave separation using Gaussian approach and triangular flow impedance approach

to be optimized. Using the LM method, for a given set of the independent and dependent variable, that is $(t, P_P(t))$, the optimizing problem is to find the parameter $K = \{A_i, M_i, C_i, i = 1$ to $N\}$ of the model curve $G(K, t)$, in such a way that the sum of least squares of the deviations $S(K)$ is minimized for a given set of k empirical pairs of independent and dependent variables, as shown in (3):

$$\hat{P} \in \operatorname{argmin}_p S(K) \equiv \operatorname{argmin}_p \sum_{i=1}^k P_P(t_i) - P_M(K_i, t_i)^2 \quad (2)$$

After obtaining $G(K, t)$, the Gaussian curves were sorted from 1 to N , based on the mean location value (M_i). The curve with the least value of M_i was numbered as 1, and the highest value of M_i was the N^{th} curve. Value of N depends on limiting maximum error ($|P_P(t) - G(K, t)|$), code execution time (Loop Time) and the sum of least square error ($\sum |P_P(t) - G(K, t)|^2$). In this work, we have considered $N = 8$, $\{|P_P(t) - G(K, t)| < 3\%$, Loop Time (Sampling Rate = 1 kHz) < 1 s}. Once the individual Gaussian energies are made available, the following expression (3), (4) are followed for separating forward and backward pressure waves.

$$P_B(t) = \frac{1}{2} \times \left(DC_{OFF} + \sum_{i=1}^N A_i e^{-\frac{1}{2} \times \frac{(t-M_i)^2}{C_i^2}} \right) \quad (3)$$

$$j = 1; \text{ if } SO_{LOC} \text{ of } P(t) < SBP_{LOC} \text{ of } P(t)$$

$$j = 2; \text{ if } SO_{LOC} \text{ of } P(t) > SBP_{LOC} \text{ of } P(t)$$

Where, SO_{LOC} is the shoulder point of $P(t)$, and SBP_{LOC} is the time location of SBP of $P(t)$. DC_{OFF} is the DC offset that was initially removed before applying the multi-Gaussian model. $P_B(t)$ is the backward wave, and $P_F(t)$ is the forward wave. DC

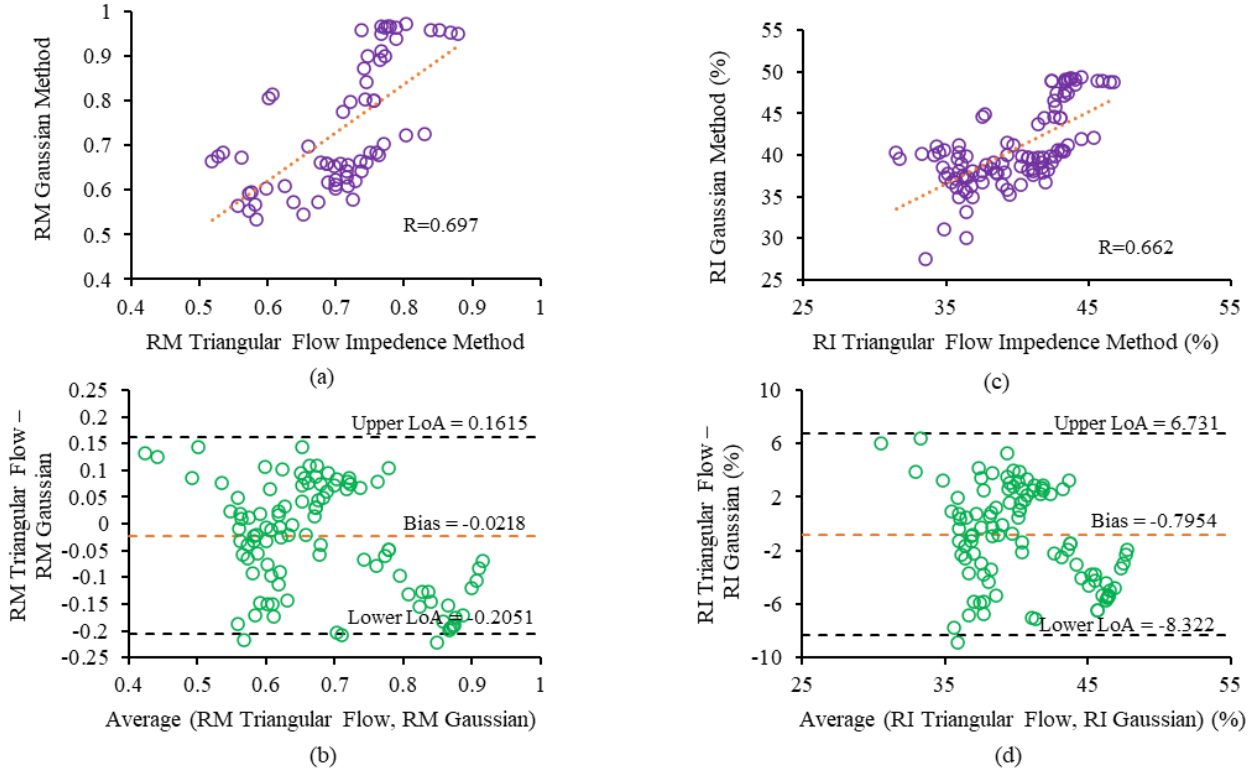


Fig.3. (a)-(b) Correlation plot and Bland Altman plot for RM of multi-Gaussian approach against RM of triangular flow velocity approximated method, (c)-(d) Correlation plot and Bland Altman plot for RI of multi-Gaussian approach against RI of triangular flow velocity approximated method.

offset is equal to the DBP value of $P(t)$. Finally, forward wave can be obtained as in (4). The separation of waves is illustrated in Fig.1.

$$P_F(t) = P(t) - P_B(t) \quad (4)$$

B. Triangular Flow Velocity Impedance Approach

This approach is based on the characteristic impedance method introduced by Westerhof et al. [10] in 1972 using flow velocity waveforms. But instead of using measured flow velocity waveforms, a triangular approximated morphology replaces measured flow velocity, as described elsewhere [16]. By doing so, this method becomes a single pulse waveform-based technique. The peak of the triangle coincides with the peak of flow wave velocity and is derived from the inflection point of the pressure wave itself. The base of the triangle corresponds to the ejection period of the ventricle, that is, from the start of the pressure cycle to the incisura. In a reflection-free infinitely long elastic tube, Z_C is defined as the ratio of pressure to flow velocity, and Z_C is approximated to input impedance (Z_0) by averaging 4 to 10 harmonics of pressure to flow velocity ratio in the frequency domain. Once Z_0 is calculated, combining it with water hammer equations, we get, $P_F = 0.5(P(t) + Z_C Q_m(t))$ and $P_B = 0.5(P(t) - Z_C Q_m(t))$ where $Q_m(t)$ is the modelled flow velocity waveform.

The reflection indices to compare the performance of the multi-Gaussian approach with this method are Reflection Magnitude (RM) and Reflection Index (RI). RM is defined as the ratio of pulse pressure of backward wave to pulse pressure of forward wave. RI is defined as the ratio of pulse pressure of

backward wave to total pulse pressure of backward and forward wave.

C. Virtual Subject Database

The multi-Gaussian modelling approach was verified on a simulated virtual subject database based on the 1D computational model of the arterial system using the spectral/hp-element framework Nektar++ [18]. The database [19] contains pulse waves representative of a healthy subject whose hemodynamic parameters (age-related trends) are varied to create virtual subjects for in-silico evaluation of haemodynamics and pulse wave indices. We have selected a subset of 105 virtual subjects from the database that has 30-35 cardiac cycles of each Type-A, Type-B and Type-C wave [20] with an age range of 25 – 75 years. The subset includes 95 normotensives (SBP: 90 – 140 mmHg, DBP: 60 – 100 mmHg) and 10 hypertensives (SBP > 140 mmHg and DBP > 100 mmHg) subjects. The mean SBP = 117.47 ± 13.04 mmHg and DBP = 71.31 ± 6.83 mmHg for the selected set.

III. RESULTS AND DISCUSSIONS

A. Error Analysis

On comparing the derived forward and backward waves using the multi-Gaussian approach with corresponding separated waves from the triangular flow velocity approximated impedance method, the root mean square error (RMSE) was found to be 1.31 ± 1.14 mmHg for 105 subjects. A bar chart of RMSE is illustrated in Fig.2(a). It was observed that 79% of the subjects had an RMSE of 2 mmHg and less, and only 8% of the subjects had an RMSE greater than 3 mmHg. Since this method is dependent on the pulse waveform

morphology, the RMSE for each category of the waveform (Type A, type B and Type C) was also calculated. For Type A RMSE was 1.91 ± 1.20 mmHg, for Type B it was 0.88 ± 0.88 mmHg and for Type C, it was 1.39 ± 1.20 mmHg. Type B waveforms are better performing in terms of RMSE against the triangular flow velocity impedance method.

B. Statistical Analysis – RM and RI

Regression and Bland Altman plots for RM and RI are shown in Fig.3(a) – (d). A statistically significant correlation ($r > 0.66$, $p < 0.0001$) was observed for RM and RI of the multi-Gaussian approach against the triangular flow velocity impedance method over the entire data set of 105 subjects. Theoretically, the maximum value of RM should be less than or equal to 1 and that of $RI < 50\%$, implying, the reflection wave must be equal to the forward wave or less than that in magnitude. The exact inference was observed in the 105 subjects as well, where the maximum reported RM for the multi-Gaussian approach was 0.972 and the maximum RM for the triangular flow velocity approach being 0.879. The multi-Gaussian approach was able to estimate RM for a range of 0.35 to 0.97 (RI: 27.53% to 49.29%) and of the triangular flow velocity approach for a range of 0.45 to 0.87 (RI: 31.48% to 46.80%). Bland-Altman plot reveals a scattered graph with no clear trend of systemic progression of errors. The bias for RM between the two methods was -0.0218, with acceptable confidence intervals (CIs) between 0.161 and -0.205. The bias for RI was -0.795%, with CIs between 6.73% and -8.32%.

C. Limitations and Future Works

Being a pilot study of the method, only virtual subject's data was utilized to prove the concept. Later, this needs to be validated with in-vivo data. A practical challenge with in-vivo study is simultaneous pressure and flow measurement at the same arterial site. For the same reasons, there is a need for methods that only requires a single pulse waveform for wave separation analysis. The algorithm needs to be explored further by incorporating a weighted Gaussian approach and reflection site calculation. The algorithm can only show a cumulative effect of all the reflections combined rather than individual reflections.

IV. CONCLUSION

This work has demonstrated a new method to separate forward and backward waves from the pulse waveform. The RM and RI were compared against the triangular flow velocity impedance method and found a statistically significant correlation. The novelty of the method lies in the fact that only a single pulse waveform is required for the decomposition analysis without the need for any modelled or measured flow velocity waveform. The method was validated across a wide range of BP and on different types of wave morphologies.

REFERENCES

- [1] J. Joseph *et al.*, "Arterial compliance probe for cuffless evaluation of carotid pulse pressure," *PLoS One*, vol. 13, no. 8, p. e0202480, 2018.
- [2] A. P. Avolio *et al.*, "Role of pulse pressure amplification in arterial hypertension: Experts' opinion and review of the data," *Hypertension*, vol. 54, no. 2, pp. 375–383, 2009.
- [3] K. S. Tang, E. D. Medeiros, and A. D. Shah, "Wide pulse pressure: A clinical review," *J. Clin. Hypertens.*, vol. 22, no. 11, pp. 1960–1967,

- 2020.
- [4] P. Zamani *et al.*, "Pulsatile Load Components, Resistive Load and Incident Heart Failure: The Multi-Ethnic Study of Atherosclerosis (MESA)," *J. Card. Fail.*, vol. 22, no. 12, pp. 988–995, 2016.
- [5] P. Zamani *et al.*, "Reflection magnitude as a predictor of mortality the multi-ethnic study of atherosclerosis," *Hypertension*, vol. 64, no. 5, pp. 958–964, 2014.
- [6] J. A. Chirinos, "Deep Phenotyping of Systemic Arterial Hemodynamics in HFpEF (Part 2): Clinical and Therapeutic Considerations," *J. Cardiovasc. Transl. Res.*, vol. 10, no. 3, pp. 261–274, 2017.
- [7] S. T. Chiesa *et al.*, "Carotid artery wave intensity in mid-to late-life predicts cognitive decline: The Whitehall II study," *Eur. Heart J.*, vol. 40, no. 28, pp. 2300–2309, 2019.
- [8] C. Manisty *et al.*, "Wave Reflection Predicts Cardiovascular Events in Hypertensive Individuals Independent of Blood Pressure and Other Cardiovascular Risk Factors. An ASCOT (Anglo-Scandinavian Cardiac Outcome Trial) Substudy," *J. Am. Coll. Cardiol.*, vol. 56, no. 1, pp. 24–30, 2010.
- [9] P. Segers *et al.*, "Limitations and pitfalls of non-invasive measurement of arterial pressure wave reflections and pulse wave velocity," *Artery Res.*, vol. 3, no. 2, pp. 79–88, 2009.
- [10] N. Westerhof, P. Sipkema, G. C. V. Den Bos, and G. Elzinga, "Forward and backward waves in the arterial system," *Cardiovasc. Res.*, vol. 6, no. 6, pp. 648–656, 1972.
- [11] K. H. Parker, "An introduction to wave intensity analysis," *Med. Biol. Eng. Comput.*, vol. 47, no. 2, pp. 175–188, 2009.
- [12] A. P. G. Hoeks, J. M. Willigers, and R. S. Reneman, "Effects of assessment and processing techniques on the shape of arterial pressure-distension loops," *J. Vasc. Res.*, vol. 37, no. 6, pp. 494–500, 2000.
- [13] R. Manoj, R. Kiran, P. M. Nabeel, J. Joseph, and M. Sivaprakasam, "A Bi-modal Probe Integrated with A-mode Ultrasound and Force Sensor for Single-site Assessment of Arterial Pressure-Diameter Loop," in *IEEE International Symposium on Medical Measurements and Applications (MeMeA)*, 2020, pp. 1–6.
- [14] P. M. Nabeel *et al.*, "Local Pulse Wave Velocity: Theory, Methods, Advancements, and Clinical Applications," *IEEE Rev. Biomed. Eng.*, vol. PP, no. c, pp. 1–1, 2019.
- [15] J. G. Kips *et al.*, "Evaluation of noninvasive methods to assess wave reflection and pulse transit time from the pressure waveform alone," *Hypertension*, vol. 53, no. 2, pp. 142–149, 2009.
- [16] B. E. Westerhof, I. Guelen, N. Westerhof, J. M. Karemaker, and A. Avolio, "Quantification of wave reflection in the human aorta from pressure alone: A proof of principle," *Hypertension*, vol. 48, no. 4, pp. 595–601, 2006.
- [17] G. Swamy, N. B. Olivier, and R. Mukkamala, "Calculation of Forward and Backward Arterial Waves by Analysis of Two Pressure Waveforms," *IEEE Trans. Biomed. Eng.*, vol. 57, no. 12, pp. 2833–2839, 2010.
- [18] C. D. Cantwell *et al.*, "Nektar++: An open-source spectral/hp element framework," *Comput. Phys. Commun.*, vol. 192, pp. 205–219, 2015.
- [19] P. H. Charlton, J. Mariscal Harana, S. Vennin, Y. Li, P. Chowienzyk, and J. Alastruey, "Modeling arterial pulse waves in healthy aging: a database for in silico evaluation of hemodynamics and pulse wave indexes," *Am. J. Physiol. Heart Circ. Physiol.*, vol. 317, no. 5, pp. H1062–H1085, 2019.
- [20] J. P. Murgu, N. Westerhof, J. P. Giolma, and S. A. Altobelli, "Aortic Input Impedance in Normal Man: Relationship to Pressure Wave Forms," *Circ. J.*, vol. 62, no. 1, pp. 105–116, 1980.